Journal of Membrane Science 372 (2011) 182–190

Contents lists available at ScienceDirect

Journal of Membrane Science

journal homepage: www.elsevier.com/locate/memsci

Composite capillary membrane for solvent resistant nanofiltration

S.M. Dutczak[a], M.W.J. Luiten-Olieman[b], H.J. Zwijnenberg[c], L.A.M. Bolhuis-Versteeg[d], L. Winnubst[b], M.A. Hempenius[e], N.E. Benes[a], M. Wessling[a,1], D. Stamatialis[d,*]

[a] Institute for Nanotechnology MESA+, University of Twente, Faculty of Science and Technology, Membrane Technology Group, P.O. Box 217, NL-7500 AE Enschede, The Netherlands
[b] Institute for Nanotechnology MESA+, University of Twente, Faculty of Science and Technology, Inorganic Membranes, P.O. Box 217, 7500 AE Enschede, The Netherlands
[c] European Membrane Institute Twente, University of Twente, Faculty of Science and Technology, Membrane Technology Group, P.O. Box 217, 7500 AE Enschede, The Netherlands
[d] Institute for Biomedical Technology and Technical Medicine MIRA, University of Twente, Faculty of Science and Technology, Membrane Technology Group, P.O. Box 217, NL-7500 AE Enschede, The Netherlands
[e] Materials Science and Technology of Polymers Faculty of Science and Technology, University of Twente, P.O. Box 217, NL-7500 AE Enschede, The Netherlands

ARTICLE INFO

Article history:
Received 19 September 2010
Received in revised form 4 December 2010
Accepted 31 January 2011
Available online 4 February 2011

Keywords:
Solvent resistant nanofiltration
Capillary membrane
Poly (dimethylsiloxane)
Crosslinking
Composite membrane
Styrene oligomers

ABSTRACT

Solvent resistant nanofiltration (SRNF) is a membrane separation process allowing for an efficient separation of small molecules of 200–1000 g mol^{-1} from organic solvents. The application of SRNF in industry applications is currently hindered by a limited choice of SRNF membranes and configurations. Despite clear advantages of capillary membranes (high surface to volume ratio, no spacers required and therefore more compact and simpler modules can be built), commercial SRNF membranes are almost exclusively produced in a spiral wound form. In this work, we prepare and study SRNF composite capillary membranes made of an α-alumina support and a selective poly (dimethylsiloxane) (PDMS) top layer. We combine the advantages of a ceramic support such as high mechanical, thermal and chemical stability with very good separation properties of the PDMS coating. All composite membranes are systematically investigated including: permeation experiments (permeance/molecular weight cut-off, MWCO) using a high pressure set-up and study of morphology using SEM imaging. The prepared composite capillary membranes are stable for at least 40 h in toluene and have MWCO of 500 Da.

1. Introduction

Solvent resistant nanofiltration (SRNF) is an energy-efficient separation process with high potential in many branches of industry, ranging from petro-chemistry [1] to pharmaceuticals [2–6]. SRNF is a relatively new membrane process capable of effective separation of molecules in the range of 200–1000 g mol^{-1} in various organic solvents. Most of the SRNF membranes reported in the literature are either asymmetric integrally skinned made of polyimides (PI) [7] or composites comprising of a thin poly (dimethylsiloxane) (PDMS) separating layer on a poly acrylonitrile (PAN) [8–15] or PI porous support [16]. In order to improve chemical resistance of PI membranes to organic solvents, a diamine crosslinking step has been applied, too [17,18]. The crosslinking can be performed as a post casting process or be incorporated into the phase inversion process itself [19].

In the industry, the majority of the organic solvent nanofiltration processes use commercial polymeric membranes which are exclusively in a spiral wound form (e.g. SolSep NF 030306; MET Starmem^{TM}). The MPS-50 has been applied for example in pharmaceutical manufacturing for solvent exchange [4] or for the recovery of organometallic complexes from organic solvents [20] but it is not available any more (its production was discontinued a few years ago). The Starmem^{TM} PI membranes have been used to separate phase transfer catalyst (PTC) from toluene [21,22] and for the recovery of dewaxing solvents (e.g. toluene) from dewaxed lube oil filtrates in petrochemistry [23]. A recent publication also showed, that SolSep membranes can be successfully used in different separation and purification stages in the biodiesel production process [24].

It is well known that a membrane in hollow fibre (HF) or capillary form has some advantages over membranes in a flat sheet configuration. A capillary/HF membrane provides a high surface to volume ratio, does not require spacers and thus enables the design of more compact and much simpler modules. Unfortunately, there are neither SRNF hollow fibres nor capillary membranes commercially available and literature reports very little on this topic. Only recently Loh et al. developed polyaniline (PANI) hollow fibres with good stability in di-methyl formamide and acetone [25].

It is obvious, that there is need to develop SRNF hollow fibre/capillary membranes to make SRNF a more attractive and more competitive separation technique. To this end, in this work

* Corresponding author. Tel.: +31 53 4894675; fax: +31 53 489 4611.
E-mail address: d.stamatialis@utwente.nl (D. Stamatialis).
[1] Present address: RWTH Aachen University, Chemische Verfahrenstechnik (CVT), 52064 Aachen, Germany.

0376-7388/$ – see front matter © 2011 Elsevier B.V. All rights reserved.
doi:10.1016/j.memsci.2011.01.058

we prepare composite capillary membranes, made of a commercial Hyflux InoCep M20 α-alumina capillary support and a selective poly (dimethylsiloxane) (PDMS) top layer. In contrast to polymeric support membranes [6,26] ceramic materials do not compact at high pressures and are inert to virtually all organic solvents making them excellent candidates for membrane supports. As a separation layer we chose PDMS due to its well established position in SRNF. To the best of our knowledge, this work is the first reporting composite α-alumina/PDMS capillary membranes for SRNF. Other studies developed capillary/hollow fibres or tubular membranes based on a PDMS selective layer but only for pervaporation or VOC removal [27–30]. All composite membranes are systematically investigated including permeation experiments (permeance/MWCO) using a high pressure cross flow set-up and study of morphology using SEM imaging.

2. Experimental

2.1. Materials

InoCep™ M20 ceramic capillaries (I.D. 2.8 mm, O.D. 3.8 mm) made of α-alumina were purchased from HyFlux Ltd. (The Netherlands). The pore size on the inside of the capillary was 20 nm and 800 nm on the outside (as reported by the manufacturer). Toluene (for analysis) was purchased from Merck (The Netherlands), styrene (Reagent Plus ≥99%), *sec*-buthyl lithium solution (1.4 M in cyclohexane), were purchased from Sigma–Aldrich (The Netherlands) and used as supplied. General Electric PDMS RTV 615 kit was purchased from Permacol B.V. (The Netherlands). The silicone kit consisted of two components; a vinyl terminated pre-polymer (RTV-A) and a Pt-catalyzed cross-linker (RTV-B) containing a poly hydrosilane component. A two component epoxy resin Araldite® 2014-1 obtained from Viba (The Netherlands) was used as potting in module preparation with membranes having the selective layer on the outside of the capillary. Sauereisen electrical cement No. DW-30 was purchased from Sepp Zeug Gmbh & Co. Kg Adhesive Cements (Germany), and used as a potting material for modules where the selective layer was on the inside of the capillary.

2.2. Preparation of the coating solution

RTV 615 pre-polymer (RTV-A) was dissolved in toluene. The solution was first brought to 60 °C under reflux and stirring, and then the crosslinking component (RTV-B) was added. The concentration of PDMS solution was 15% (w/w). After addition of the RTV-B component, the exact timing of the crosslinking reaction was started. The crosslinking reaction was carried out in three steps. In the first step, the temperature of the reaction was kept at 60 °C for 150 min and then the temperature was decreased to 50 °C. The reaction continued till the solution reached a viscosity of about 100 mPa s. In the next step, the viscous solution was diluted with toluene to 7.5% (w/w) and the crosslinking was continued at 60 °C till the solution reached a viscosity of about 100 mPa s. Finally in step 3, the solution was diluted with toluene to 3.7% (w/w) and reaction was continued at 60 °C until a desired viscosity was reached. The solution of the pre-crosslinked PDMS was cooled down in an ice bath to stop the reaction. All viscosity measurements were performed at 25 °C on a Brookfield DV-II+ Pro viscometer using a spindle nr-61 (Ø18.9 mm) and glass cylinder (Ø26 mm).

2.3. Composite membrane preparation

The composite membranes were prepared in an ISO-6 class dust free room. The membranes with the selective layer on the outside of the support were prepared by dip-coating in the pre-crosslinked PDMS/toluene solution. The coating was performed using an automated set-up adjusted to an immersion/pull up velocity of 0.9 cm/s and a contact time of 30 s. The membranes with the selective layer on the inside of the support were prepared using a communicating vessel principle. The capillary support was fixed in a vertical position and its bottom end was connected by a flexible (polyurethane) hose with the bottom part of a vessel containing a PDMS coating solution. The change of the level of the PDMS coating solution inside the capillary support was regulated by rising-lowering the vessel with the PDMS coating solution. The filling/emptying velocity and the contact time were controlled by the automated set-up at 0.9 cm/s and at 30 s respectively. In both cases, a single coating was performed after which the membranes were left at room temperature for 30 min to evaporate the solvent. Subsequently, the coated tubes were put into an oven at 60 °C for 8 h to complete the crosslinking reaction. The produced membranes coated on the outside are named M800/*X* whereas those coated on the inside M20/*X*, where *X* is the viscosity (in mPa s) of PDMS solution used for coating.

2.4. Module preparation

The composite membranes were potted in cross-flow stainless steel modules. Each module contained one capillary of 155 mm active length. The membrane area of each M800/*X* module was 1.86×10^{-3} m^2 and of the M20/*X* was 1.36×10^{-3} m^2. Araldite® 2014-1 was used as a potting material for membranes M800/*X*. The resin was allowed to set at room temperature for minimum 24 h before using the module for permeation experiments. The M20/*X* membranes were potted with Sauereisen electrical cement No. DW-30 cured at room temperature for minimum 48 h. If the Araldite® 2014-1 is used there, the membranes crack due to the mechanical stress caused by the slight swelling of the potting in toluene. For the M800/*X* membranes, it seems that the PDMS layer (coating) between Araldite® and the α-alumina capillary absorbs the mechanical stress due to resin swelling thus preventing membrane cracking.

2.5. MWCO determination

2.5.1. Polystyrene synthesis

Polystyrene (PS) of broad molecular weight (MW) was synthesized by anionic living polymerization. The polymerization was carried out in a 2 l three neck round bottom flask equipped with magnetic agitator, dropping funnel, vertical condenser and a rubber septum. To ensure an oxygen and moisture free reaction environment, the set up was purged continuously with a slow stream of dry nitrogen. The temperature of the polymerizing solution was maintained below 30 °C all the time.

In the reaction flask, containing 500 g of toluene, 200 ml of 1.4 M sec-butyllithium (0.28 mol) was injected through the septum. Next, 71.8 g (0.69 mol) styrene dissolved in 90 g of toluene was added within 8 min into the *sec*-butyllithium toluene solution. The reaction mixture was stirred for 4 min and afterwards, 8.4 ml (0.21 mol) of methanol was injected to quench 75% of the growing polymer chains. Directly afterwards 71.8 g (0.69 mol) styrene dissolved in 90 g of toluene was added during 3.5 min to the polymerizing solution. The PS solution was stirred for an additional 2 h at room temperature and quenched with 10 ml of methanol.

After quenching, the synthesised PS was purified by partial evaporation of solvents in a rotary evaporator followed by removal of the lithium metoxide by washing the PS oligomers with distilled water. The washing was repeated several times until the water phase reached neutral pH (removal of LiOH). To complete the purification process, the rest of the solvent was evaporated first in a rotary evaporator and next in a nitrogen box at room temperature. A 0.3% (w/w) broad range MW PS solu-

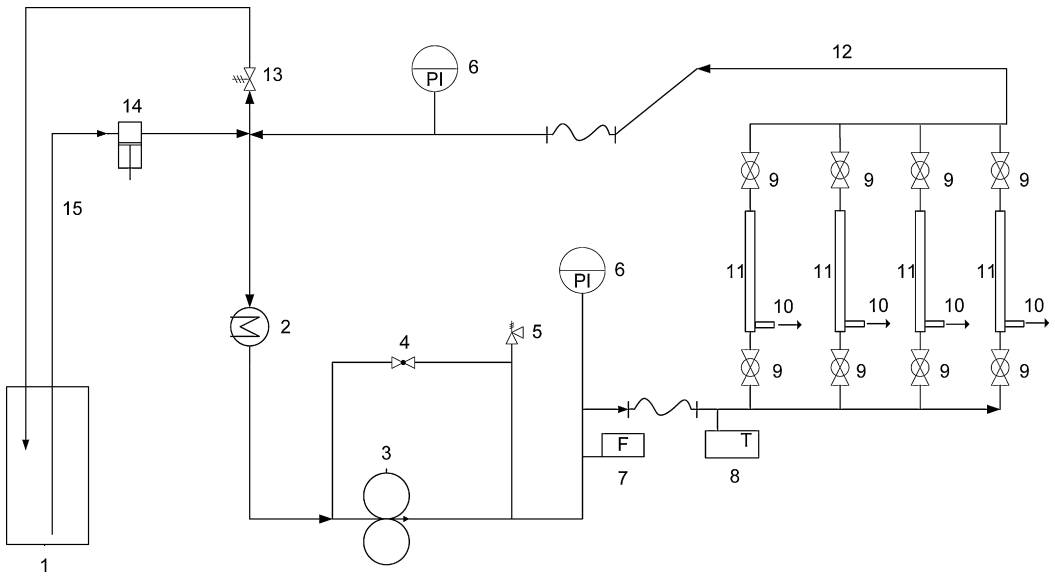

Fig. 1. High pressure permeation set up: (1) feed vessel, (2) heat exchanger, (3) gear pump, (4) bypass ball valve, (5) pressure relief, (6) pressure indicator, (7) flow meter, (8) temperature controller, (9) ball valves, (10) permeate line, (11) membrane modules, (12) retentate line, (13) back pressure valve, (14) HPLC pump, (15) feed line.

tion in toluene was used for the filtration experiments to obtain MWCO curves.

2.5.2. Determination of PS oligomers retention

The concentration of the PS oligomers as a function of MW in the feed and permeate stream was determined by GPC chromatography. For this we used "Agilent Technologies 1200 Series" GPC system equipped with the refractive index detector "Shodex RI-71". The column used for separation of PS oligomers was PSS SDV with porosity 1000 Å. As a mobile phase analytical grade toluene was used.

Similar to the method developed by Schock et al. for measurement of the MWCO of ultrafiltration membranes [31], the GPC analysis resulted in a single lumped peak for both permeate and feed samples. The data was then processed by the GPC software (Win GPC Unity) in order to obtain retention curves.

The membrane retention R, for the PS oligomers was calculated from permeate and feed samples with the following equation:

$$R_{i-PS}(\%) = \left(1 - \frac{C_{P,i}}{C_{F,i}}\right) \times 100 \quad (1)$$

where $C_{P,i}$ and $C_{F,i}$ are the concentrations of the individual PS oligomers in the permeate and the feed stream respectively.

2.6. Scanning electron microscopy (SEM) characterization

Composite membranes were fractured in liquid nitrogen. The samples were then mounted in holders, dried in vacuum oven at 30 °C for 12 h and sputtered with gold using a Blazers Union SCD 040 sputtering device (4 min, current 13 mA). SEM micrographs were taken using a Jeol JSM5600LV scanning electron microscope at 5 kV.

2.7. Gas permeation measurements and determination of PDMS layer thickness

Gas permeation measurements of the composite capillary membranes were performed in an automized constant volume/variable pressure set up (see details elsewhere [32]). The gas permeance values were calculated based on a pressure increase in a calibrated constant volume at the permeate side. The temperature during all measurements was maintained at 30 °C. From gas permeation values the effective PDMS layer thickness (l_{eff}) was calculated. It was assumed that PDMS intrinsic permeability of N_2 equals 280 Barrers and CO_2 3200 Barrers [33]. The obtained l_{eff} was compared with the PDMS thickness obtained by SEM observation (l_{SEM}) to estimate the extent of the pore intrusion (l_{intr}):

$$l_{intr} = l_{eff} - l_{sem} \quad (2)$$

The l_{SEM} was obtained from SEM images of cross sections of at least three different membranes per case. The average PDMS thickness per sample was obtained from five SEM images per cross section.

2.8. Permeation experiments

All permeation experiments were performed in a custom made cross-flow high pressure permeation set-up (Fig. 1) in a total recycle mode. The set-up was equipped with an HPLC pump which pressurizes the system up to 40 bar. A gear pump was used for circulation and equipped with frequency inverter allowing precise control over the cross flow velocity. All permeation experiments were performed at a crossflow velocity of the feed solution above 2 m/s. The membranes M800/*X* have been tested outside-in and the M20/*X* inside-out. The temperature of the feed solution was controlled at 18 °C. The flux through the membrane (J, in $l\,m^{-2}\,h^{-1}$) was calculated using the following equation:

$$J = \frac{V}{A \times t} \quad (3)$$

where V is the permeate volume (l), A the membrane area (m^2) and t is the permeation time (h). The permeance coefficient, P ($l\,m^{-2}\,h^{-1}\,bar^{-1}$), was calculated from the slope of the flux versus trans membrane pressure (TMP) graph:

$$P = \frac{J}{\Delta P} \quad (4)$$

3. Results and discussion

3.1. Preparation of PDMS coating solutions

In order to prepare a good quality composite membrane it is crucial to prepare a PDMS coating solution of well-defined properties. It is generally known that using lower concentrations one

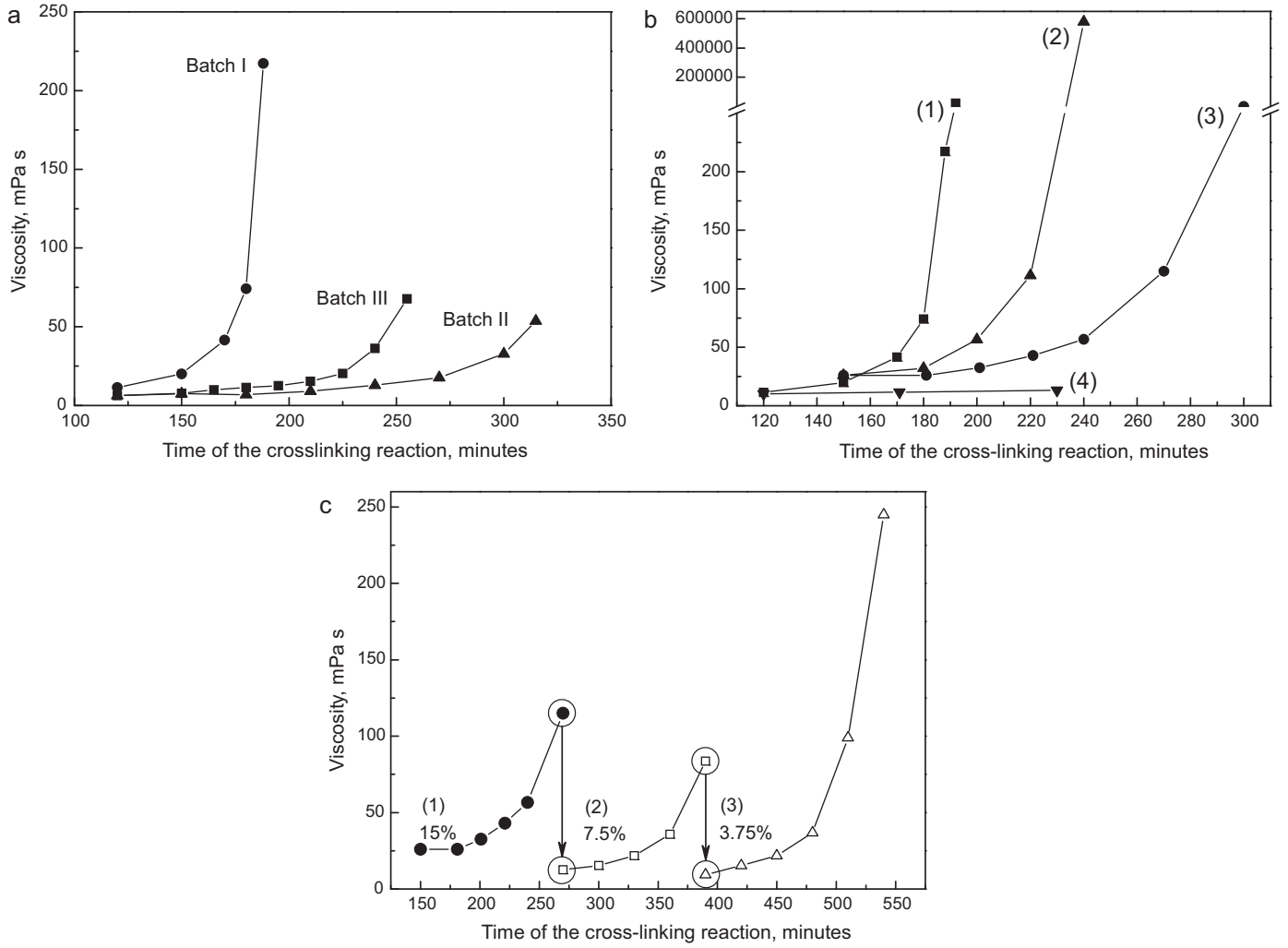

Fig. 2. Crosslinking of PDMS coating solutions: (a) difference between PDMS batches – 15% (w/w) toluene solution, (b) influence of temperature on viscosity of PDMS coating solution – 15% (w/w) toluene solutions: (1) constant $T = 60\,^{\circ}C$, (2) 150 min at $T = 60\,^{\circ}C$ then the temperature lowered to $T = 55\,^{\circ}C$, (3) 150 min at $T = 60\,^{\circ}C$ then the temperature lowered to $T = 50\,^{\circ}C$, (4) 150 min at $T = 60\,^{\circ}C$ then the temperature lowered to $T = 40\,^{\circ}C$ (c) effect of dilution on viscosity of PDMS coating solution: (1) 15%, (2) 7.5%, (3) 3.75%. The measurement error for all results presented in figures (a), (b) and (c) is less than 10%.

can fabricate thin selective layers, however, the viscosity of the PDMS solution should be sufficient to make a defect free coating. Diluted PDMS solutions have very low viscosity and are not suitable to be applied directly as coatings. To achieve a high solution viscosity at low PDMS concentrations it is necessary to pre-crosslink the coating solution [11].

Following the pre-crosslinking procedure described by Stafie et al. [10,12] we prepared several 15% (w/w) toluene/PDMS solutions. Fig. 2a shows viscosity changes as a function of crosslinking reaction time for three different factory batches of GE RTV615 silicone. Our results suggest that although all three batches are within the factory specification, the behaviour during crosslinking reaction varies greatly. One can see that for Batch I and Batch II the time difference where a sharp increase in viscosity occurs, is as much as 150 min. Despite such significant variations between batches it is possible to obtain PDMS solutions of desired viscosity by tuning the reaction time for each batch separately. Fig. 2b presents the change of the viscosity of a 15% (w/w) PDMS coating solution versus crosslinking time for different reaction conditions. All curves presented in Fig. 2b were obtained using the silicone batch I (see Fig. 2a, batch I). Case 1 shows the change of viscosity of the PDMS solution, cross-linked at constant 60 °C. Here, the viscosity increases up to 6 times in only 20 min between 170 and 190 min of the reaction time. In case 2 after 150 min of crosslinking at 60 °C we decreased the temperature to 55 °C. As a result the viscosity increase occurs later and is somewhat less sharp. When after 150 min of crosslinking at 60 °C the temperature is decreased to 50 °C (Fig. 2b, case 3) the change of viscosity is less dramatic. If one decreases the crosslinking reaction temperature earlier than 150 min, or uses temperatures lower than 50 °C, the PDMS viscosity stays below 20 mPa s for more than 300 min (see Fig. 2b, case 4). Since controlling the viscosity of a coating solution is very important to obtain a good coating quality, it seems that a better control of viscosity can be achieved at a temperature around 50 °C.

After some preliminary coating experiments with 15% (w/w) solution, we found that when the coating solution viscosity is high, we obtain a thick PDMS layer whereas when the viscosity is low we obtain membranes with high pore intrusion and defects. It is desirable to have a solution with relatively low PDMS concentration, to obtain thin selective layer, but of relatively high viscosity, to avoid pore intrusion and defects. Fig. 2c presents the viscosity change in three different phases of the crosslinking reaction. Phase (1) presents the viscosity of 15% (w/w) solution first crosslinked for 150 min at 60 °C and subsequently for 120 min at 50 °C. Next, the solution was diluted with toluene to 7.5% (w/w) and crosslinking was continued at 60 °C for 120 min (Fig. 2c, phase 2). After that the solution was again diluted with toluene to 3.75% (w/w) and the reaction continued at 60 °C (Fig. 2c, phase 3). These results show

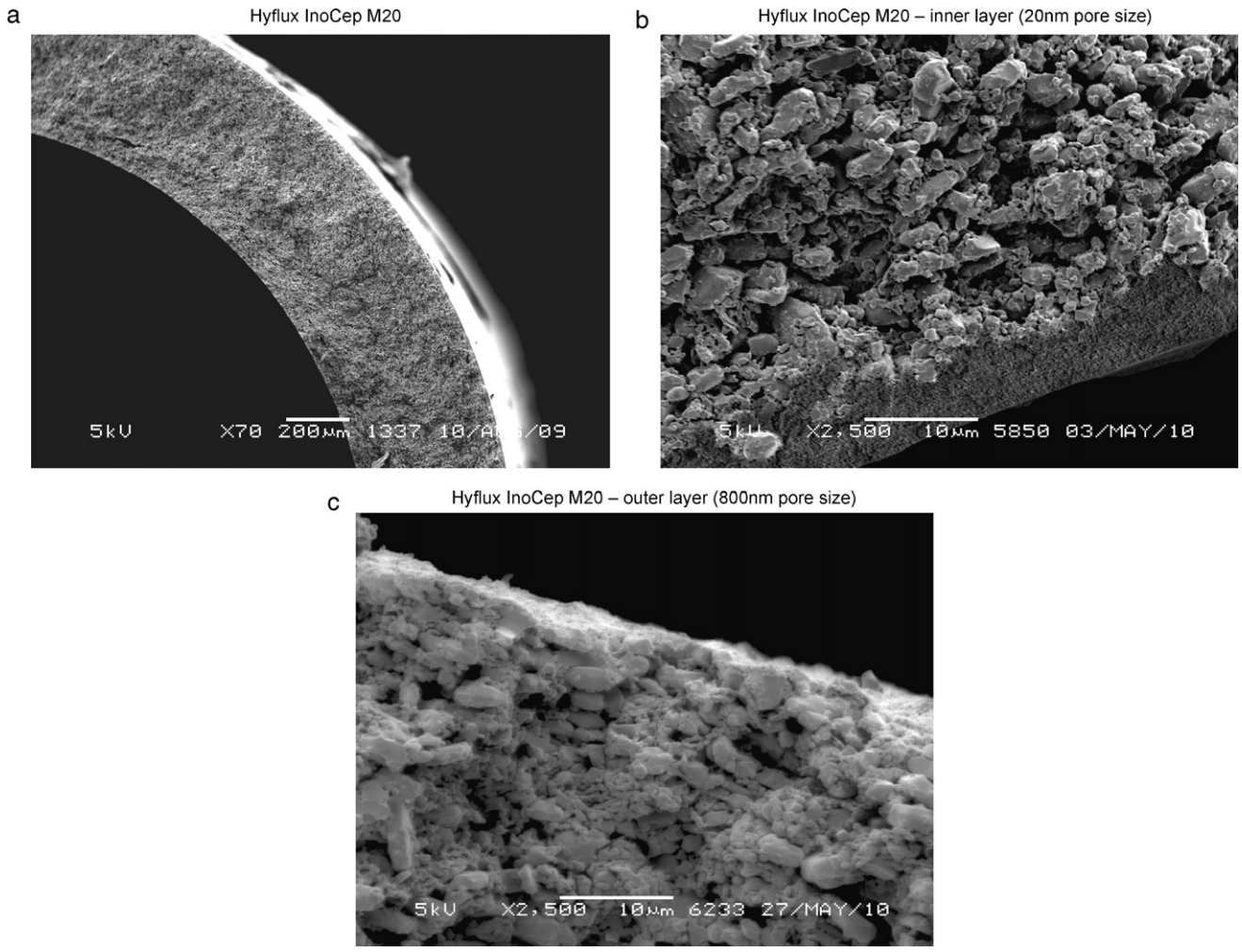

Fig. 3. Scanning electron microscopy (SEM) images of Hyflux InoCep M20 capillary support. (a) Wall cross-section, (b) cross-section of the inner layer (20 nm pore size), (c) cross-section of the outer layer (800 nm pore size).

that one can tailor precisely the viscosity of diluted solutions, even at 60 °C.

Our crosslinking results show that we can control the viscosity of the PDMS coating solution independent of the concentration. In fact, a pre-crosslinking procedure with gradual dilution enables preparation of carefully tailored PDMS solutions of various concentrations and of any viscosity between 10 and 300 mPa s. Based on the above results we selected cross-linked 3.75% (w/w) PDMS/toluene solutions with viscosities: 55, 69, 100 and 245 mPa s for the preparation of composite membranes.

3.2. Characterization of InoCep M20 Hyflux ceramic support

Fig. 3a presents a SEM image of the cross section of the Hyflux InoCep M20 support. In Fig. 3b one can see the ~5 μm denser ceramic coating with 20 nm pore size (as reported by the manufacturer) on the inside of the capillary. The outside layer of the capillary has larger pores of 800 nm pore size (as reported by the manufacturer) (see Fig. 3c).

Fig. 4 presents the flux of toluene as a function of transmembrane pressure (TMP). Within the studied pressure range (0–9 bar) the line remains straight indicating that no compaction occurs. Because of the very high flux of toluene through InoCep M20 support we were not able to apply higher pressures in our experimental set-up. The toluene permeance of the M20 capillary is $575 \pm 5\,l\,m^{-2}\,h^{-1}\,bar^{-1}$.

3.3. Optimization of ceramic/PDMS hollow fibre membrane

3.3.1. Coating on the outside (M800/X)

Table 1 presents an overview of the coating experiments. The first series of the composite membranes were prepared by dip coating on the outside of the support. In order to investigate the influence of PDMS solution viscosity on pore intrusion we used 3.75% (w/w) PDMS solutions with three different viscosities: 69,

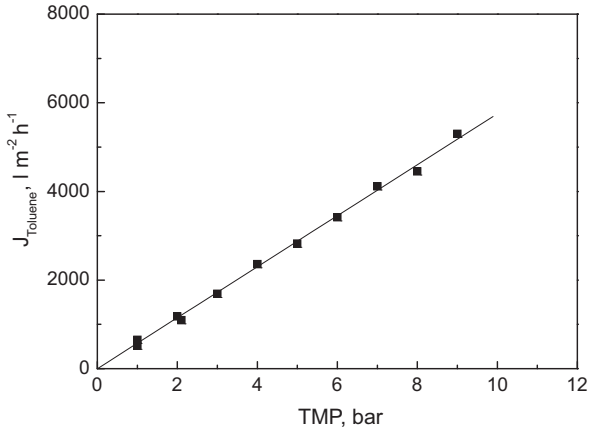

Fig. 4. Transport of toluene through Hyflux Inocep M20 support.

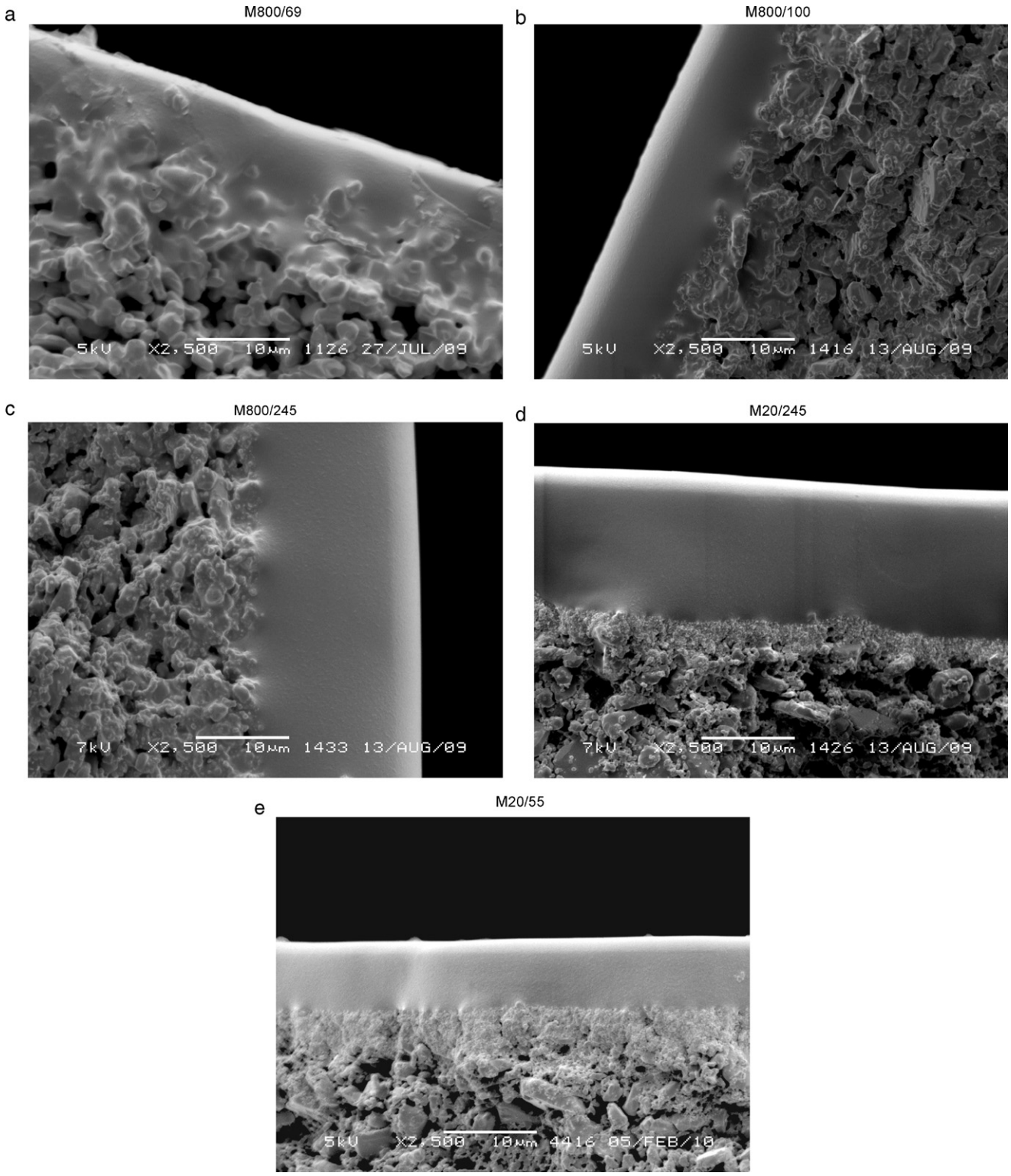

Fig. 5. Hyflux InoCep M20/PDMS composite capillary membranes: (a) M800/69, (b) M800/100, (c) M800/245, (d) M20/245, (e) M20/55.

100 and 245 mPa s (tailored as described in Fig. 2c). SEM images of cross-sections of those membranes are presented in Fig. 5a–c respectively. The thickness of the PDMS on top of the 800 nm pore size support layer (l_{SEM}) was, 6 μm for the M800/69, 10 μm for M800/100 and 18 μm for M800/245 membrane. The l_{eff}, as calculated based on N_2 permeance measurements, was 51 μm, 28 μm and 32 μm for M800/69, M800/100 and M800/245 respectively. For all prepared membranes we also calculated $\alpha CO_2/N_2$ in order to check the quality of the PDMS layer. For all M800/*X* membranes the $\alpha CO_2/N_2$ was above 10 (the ideal $\alpha CO_2/N_2$ is 11.3 [11]) showing a very good quality of the coating (see Table 1). When the coating solution viscosity was increased the coating thickness on top of the support also increased from 6 to 18 μm, whereas the estimated pore intrusion decreased from 45 to 14 μm.

Fig. 6 presents the flux of toluene as a function of pressure for the composite membranes. The error bars represent deviation between

Table 1
Characteristics of membranes and results of permeation measurements.

Code	PDMS (w/w, %)	Viscosity (mPa s)	Support pore size (nm)	l_{SEM} (μm)	l_{eff} (μm)	Estimated pore intrusion (μm)	Selectivity $\alpha CO_2/N_2$	Toluene permeance ($l\,m^{-2}\,h^{-1}\,bar^{-1}$)
M20	–	–	20	–	–	–	–	575 ± 5
M800/69	3.75%	69	800	6 ± 3	51 ± 1	45	10.6 ± 0.1	0.07 ± 0.01
M800/100	3.75%	100	800	10 ± 1	28 ± 1	18	10.0 ± 0.2	0.22 ± 0.02
M800/245	3.75%	245	800	18 ± 3	32 ± 6	14	10.3 ± 0.3	0.14 ± 0.02
M20/245	3.75%	245	20	16 ± 4	16 ± 1	0	8.4 ± 0.1	0.9 ± 0.6
M20/55	3.75%	55	20	7.3 ± 0.3	7.1 ± 0.2	0	8.4 ± 0.1	1.6 ± 0.1

the samples of the composite membranes from the same batch. The error of the permeation measurement itself is less than 1%. All M800/*X* membranes have relatively low toluene permeance. The M800/69 membrane has the largest pore intrusion resulting in the highest l_{eff} and therefore has the lowest toluene permeance. The M800/100 membrane with the lowest l_{eff} has the highest permeance. The PDMS thickness measured from SEM images for M800/100 and M800/245 (compare Fig. 5b and c) is 10 μm and 18 μm respectively and is consistent with the trend of toluene permeance for both membranes. It seems that further increase of the coating solution viscosity above 245 mPa s would produce a membrane with even lower permeance of toluene.

The results above suggest that in order to obtain a thinner PDMS layer it is necessary to use a support with smaller pore size. InoCep M20 capillaries have 20 nm pore size on the inner side, allowing the use of the same support for further optimization of composite membranes, by coating the inner surface of the capillaries.

3.3.2. Coating on the inside (M20/X)

Fig. 5d presents a cross section of a composite capillary membrane (M20/245), prepared by coating a 3.75% (w/w) PDMS toluene solution of a viscosity of 245 mPa s on the inside of the support membrane. A close examination of the SEM image does not reveal pore intrusion. The l_{eff} and l_{SEM} are in close agreement, also indicating that no significant pore intrusion occurred (see Table 1). It is nonetheless important to point out that for this membrane the $\alpha CO_2/N_2$ was ~8.4 (ideal 11.3 [34]) indicating some defects in the separation layer. One must be aware that those defects influence the gas permeation measurements leading to a slightly lower calculated PDMS thickness.

Fig. 6 presents the flux of toluene as a function of pressure for membrane M20/245. The permeance of toluene, P_{tol}, was 0.9 ± 0.6, $l\,m^{-2}\,h^{-1}\,bar^{-1}$. The low reproducibility of this membrane is probably due to a combination of two factors, high viscosity of the coating solution and applied coating technique (communicating vessel system). It seems that due to the high viscosity of the PDMS solution, control over the contact time and coating velocity is not precise, resulting in membranes with high and low permeances.

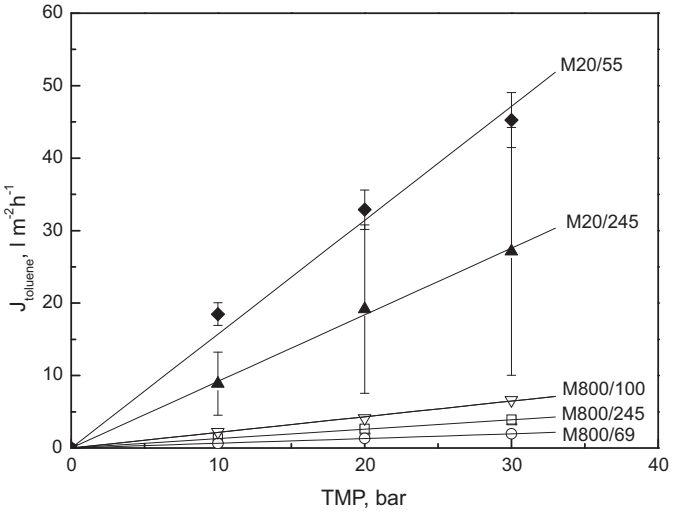

Fig. 6. Transport of toluene through alumina/PDMS hollow fibre membranes.

In order to obtain a better composite membrane with a thinner and reproducible coating we used a 3.75% (w/w) PDMS toluene solution with a viscosity of 55 mPa s. Fig. 5e presents a cross-section of this composite (M20/55) membrane. A close examination of the SEM image suggests no pore intrusion. Also, l_{eff} and l_{SEM} are similar and about 7 μm (see Table 1). The $\alpha CO_2/N_2$ of the M20/55 membranes is ~8.4 suggesting the presence of some defects in the PDMS layer. The toluene permeance of this membrane is 1.6 ± 0.1, $l\,m^{-2}\,h^{-1}\,bar^{-1}$, even higher than for the best sample of membrane M20/245. The reproducibility of the M20/55 composite membranes is considerably better as demonstrated by the small thickness deviation between the samples (see Table 1). The less viscous coating solution allows better control over the coating process resulting in much better composite membranes. The thickness of the PDMS layer of our membrane M20/55 is 7 μm and is lower than that reported for other capillary membranes for pervaporation (~10 μm) [28] and hollow fibres for VOC removal (15.4 μm) [27].

In conclusion, based on the above results, the M20/55 is the best membrane developed in this study, having low pore intrusion and the highest toluene permeance.

3.3.3. Molecular weight cut-off determination

In order to characterize the retention behaviour of the nanofiltration (NF) membranes in organic solvents one needs a series of solutes of increasing molecular weight (MW). It is also important that all the molecules have the same chemical properties and are well soluble in the solvent used. Voigt et al. [35] proposed a filtration of mixture of narrow low-MW fractions of styrene oligomers dissolved in toluene as a method for MWCO characterization of ceramic NF membranes. Later, the concept was further developed by See Toh et al. [36]. The disadvantage of the use of a mixture of commercial PS is the relatively high price of these styrene oligomers. Zwijnenberg [37] proposed therefore a method of synthesis of a broad range PS to be used for NF module testing. Since the amount of solution needed for our experiments was quite significant, we performed the synthesis of broad MW PS in our lab by means of the anionic living polymerization of styrene. This method is rather simple, leads to high yields (~95% after purification) and by varying the styrene to *sec*-butyllithium ratio allows simple adjustment of the MW of the final product. Fig. 7a (dotted line – feed) presents MW distribution of the obtained PS. The addition of small amounts of methanol, which terminates partially the growth of the chains, also results in preparation of PS fractions of 300 and 400 g/mol, thus increasing polydispersity.

The membrane M20/55, as the best one of all the membranes prepared in this study was chosen for MWCO characterization. For the retention measurements we used a 0.3% (w/w) solution of the synthesized PS oligomers. Examples of the GPC chromatograms of the feed and permeate samples are presented in the Fig. 7a. Fig. 7b presents a comparison of pure toluene and toluene/PS oligomers

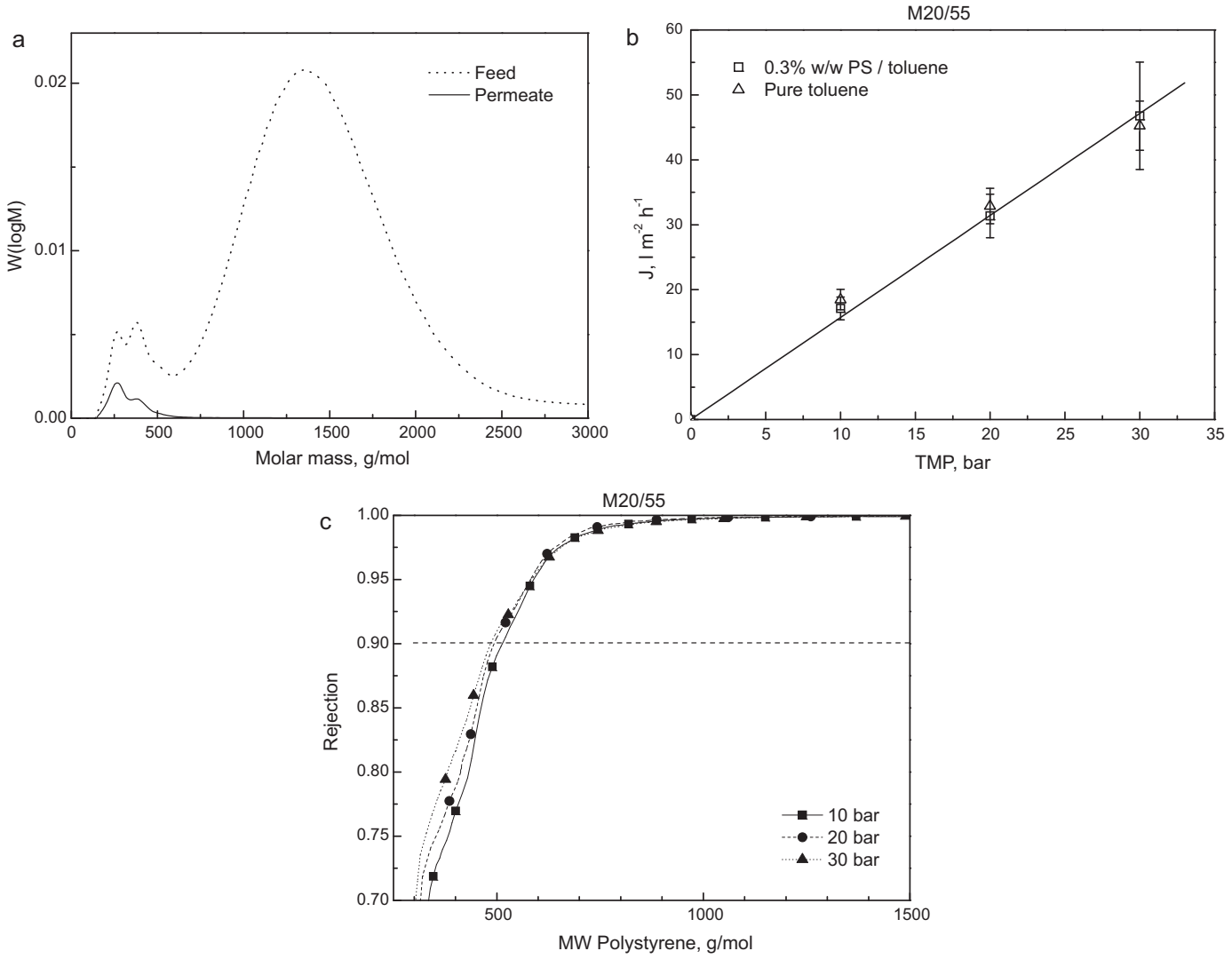

Fig. 7. Transport through M20/55 membrane: (a) molecular weight distribution of PS oligomers in the feed solution and permeate solution (b) toluene and toluene-PS transport through the membrane, (c) PS oligomer retention by the membrane.

flux as a function of TMP for this membrane. For the chosen concentration of PS oligomers and filtration parameters (cross-flow velocity above 2 m/s, stage cut below 10%) the PS oligomers/toluene flux does not differ from the pure toluene flux indicating no concentration polarization phenomena. In this pressure range no compaction occurs either. Fig. 7c presents the rejection of PS oligomers by the M20/55 membrane and shows its MWCO at about 500 Da. For this experiment, pure toluene permeation was performed for around 20 h followed by 20 h of toluene/oligostyrene filtration in a total recycle mode. The data presented in both Fig. 7b and c are obtained using the same membrane samples.

The best composite capillary membrane developed in this study, M20/55, has a toluene permeance of $1.6 \pm 0.1\,l\,m^{-2}\,h^{-1}\,bar^{-1}$ and MWCO 500 Da, and has similar permeation performance to other laboratory made silicone based composite membranes. A polyacrylonitrile-polyester/PDMS (PAN-PE/PDMS) composite reported by Vankelecom et al. [26] had a toluene permeance of $1.2\,l\,m^{-2}\,h^{-1}\,bar^{-1}$ and the PAN/PDMS composite membrane prepared by Stafie [10] had a toluene permeance of $2.0\,l\,m^{-2}\,h^{-1}\,bar^{-1}$. Comparing to commercial silicone based membranes, the MPF-50 (Koch) [6] had a toluene permeance of $1.3\,l\,m^{-2}{*}h^{-1}\,bar^{-1}$ and MWCO about 700 Da, although this membrane suffers from compaction [26] which may deteriorate membrane performance [6,38]. The permeance of our membrane is lower than an experimental PAN/PDMS membrane which was reported to have a toluene permeance of $8.2\,l\,m^{-2}\,h^{-1}\,bar^{-1}$ and 90% retention of PEG 900 [9].

When comparing to non-silicone NF membranes, a cross-linked polyimide membrane developed by See Toh et al. had a toluene permeance $3.2\,l\,m^{-2}\,h^{-1}\,bar^{-1}$ and MWCO 400 Da, based on PS oligomers rejection [17], whereas a polyimide Starmem™ membrane had a toluene permeance $1.8\,l\,m^{-2}\,h^{-1}\,bar^{-1}$ and MWCO 220 Da, based on 90% rejection of n-alkanes [6,13]. It is also important to note that the toluene permeance of our M20/55 membrane is similar to a zeolite filled PDMS mixed matrix membrane reported by Gevers et al. (toluene permeance of 1.15, $l\,m^{-2}\,h^{-1}\,bar^{-1}$ and 78% rejection of the Wilkinson catalyst (952 Da)) [39]. The same authors reported that after optimization of the coating parameters and correct pretreatment of the support (Polyimide-Matrimid®) it was possible to achieve toluene permeance of $3.3\,l\,m^{-2}\,h^{-1}\,bar^{-1}$ and 98% rejection of the Wilkinson catalyst [16].

4. Conclusions

In this work, we investigated the preparation of composite capillary membranes comprising of commercial Hyflux InoCep M20

α-alumina support and selective tailor made PDMS top layer. Our results showed that PDMS coatings on α-alumina support of 800 nm pore size did not provide a good composite membrane. Due to the large pore size, the coating solution intrudes significantly in the porous support blocking pores and decreases the toluene permeance considerably.

The best composite membrane M20/55 was prepared by coating PDMS on the inside of the α-alumina support. This membrane has stable performance for over 40 h in toluene, toluene permeance of 1.6 l m^{-2} h^{-1} bar^{-1} and MWCO of ~500 Da. Despite the relatively thick PDMS layer of 7 μm, this membrane has comparable toluene permeance with respect to various laboratory PAN/PDMS membranes with thinner PDMS layers. Further development of the composite membrane will focus on coating a PDMS layer on tailor made ceramic hollow fibres which would further improve the surface to volume ratio of the resulting module.

Acknowledgment

Dutch Technology Foundation (STW) (project no 07349) is gratefully acknowledged for the financial support.

References

[1] L.S. White, Development of large-scale applications in organic solvent nanofiltration and pervaporation for chemical and refining processes, J. Membr. Sci. 286 (2006) 26.
[2] X. Cao, X.Y. Wu, T. Wu, K. Jin, B.K. Hur, Concentration of 6-aminopenicillanic acid from penicillin bioconversion solution and its mother liquor by nanofiltration membrane, Biotechnol. Bioprocess. Eng. 6 (2001) 200–204.
[3] J.C.T. Lin, A.G. Livingston, Nanofiltration membrane cascade for continuous solvent exchange, Chem. Eng. Sci. 62 (2007) 2728–2736.
[4] J.P. Sheth, Y. Qin, K.K. Sirkar, B.C. Baltzis, Nanofiltration-based diafiltration process for solvent exchange in pharmaceutical manufacturing, J. Membr. Sci. 211 (2003) 251–261.
[5] D. Shi, Y. Kong, J. Yu, Y. Wang, J. Yang, Separation performance of polyimide nanofiltration membranes for concentrating spiramycin extract, Desalination 191 (2006) 309–317.
[6] P. Vandezande, L.E.M. Gevers, I.F.J. Vankelecom, Solvent resistant nanofiltration: separating on a molecular level, Chem. Soc. Rev. 37 (2008) 365–405.
[7] Y.H. See-Toh, F.C. Ferreira, A.G. Livingston, The influence of membrane formation parameters on the functional performance of organic solvent nanofiltration membranes, J. Membr. Sci. 299 (2007) 236–250.
[8] S. Aerts, A. Vanhulsel, A. Buekenhoudt, H. Weyten, S. Kuypers, H. Chen, M. Bryjak, L.E.M. Gevers, I.F.J. Vankelecom, P.A. Jacobs, Plasma-treated PDMS-membranes in solvent resistant nanofiltration: Characterization and study of transport mechanism, J. Membr. Sci. 275 (2006) 212.
[9] K. Ebert, J. Koll, M.F.J. Dijkstra, M. Eggers, Fundamental studies on the performance of a hydrophobic solvent stable membrane in non-aqueous solutions, J. Membr. Sci. 285 (2006) 75–80.
[10] N. Stafie, Poly(dimethyl siloxane) – based composite nanofiltration membranes for non-aqueous applications, Ph.D. thesis, University of Twente, Enschede, The Netherlands, 2004.
[11] N. Stafie, D.F. Stamatialis, M. Wessling, Insight into the transport of hexane-solute systems through tailor-made composite membranes, J. Membr. Sci. 228 (2004) 103–116.
[12] N. Stafie, D.F. Stamatialis, M. Wessling, Effect of PDMS cross-linking degree on the permeation performance of PAN/PDMS composite nanofiltration membranes, Sep. Purif. Technol. 45 (2005) 220–231.
[13] D.F. Stamatialis, N. Stafie, K. Buadu, M. Hempenius, M. Wessling, Observations on the permeation performance of solvent resistant nanofiltration membranes, J. Membr. Sci. 279 (2006) 424–433.
[14] E.S. Tarleton, J.P. Robinson, C.R. Millington, A. Nijmeijer, M.L. Taylor, The influence of polarity on flux and rejection behaviour in solvent resistant nanofiltration – experimental observations, J. Membr. Sci. 278 (2006) 318–327.
[15] E.S. Tarleton, J.P. Robinson, M. Salman, Solvent-induced swelling of membranes – measurements and influence in nanofiltration, J. Membr. Sci. 280 (2006) 442–451.
[16] L.E.M. Gevers, S. Aldea, I.F.J. Vankelecom, P.A. Jacobs, Optimisation of a lab-scale method for preparation of composite membranes with a filled dense top-layer, J. Membr. Sci. 281 (2006) 741–746.
[17] Y.H. See Toh, F.W. Lim, A.G. Livingston, Polymeric membranes for nanofiltration in polar aprotic solvents, J. Membr. Sci. 301 (2007) 3–10.
[18] K. Vanherck, P. Vandezande, S.O. Aldea, I.F.J. Vankelecom, Cross-linked polyimide membranes for solvent resistant nanofiltration in aprotic solvents, J. Membr. Sci. 320 (2008) 468–476.
[19] K. Vanherck, A. Cano-Odena, G. Koeckelberghs, T. Dedroog, I. Vankelecom, A simplified diamine crosslinking method for PI nanofiltration membranes, J. Membr. Sci. 353 (2010) 135–143.
[20] J.T. Scarpello, D. Nair, L.M. Freitas dos Santos, L.S. White, A.G. Livingston, The separation of homogeneous organometallic catalysts using solvent resistant nanofiltration, J. Membr. Sci. 203 (2002) 71–85.
[21] A. Livingston, L. Peeva, S. Han, D. Nair, S.S. Luthra, L.S. White, L.M. Freitas Dos Santos, Membrane separation in green chemical processing, Ann. N. Y. Acad. Sci. 984 (2003) 123–141.
[22] S.S. Luthra, X. Yang, L.M. Freitas dos Santos, L.S. White, A.G. Livingston, Homogeneous phase transfer catalyst recovery and re-use using solvent resistant membranes, J. Membr. Sci. 201 (2002) 65–75.
[23] L.S. White, C.R. Wildemuth, Aromatics enrichment in refinery streams using hyperfiltration, Ind. Eng. Chem. Res. 45 (2006) 9136–9143.
[24] R. Othman, A.W. Mohammad, M. Ismail, J. Salimon, Application of polymeric solvent resistant nanofiltration membranes for biodiesel production, J. Membr. Sci. 348 (2010) 287–297.
[25] X.X. Loh, M. Sairam, J.H.G. Steinke, A.G. Livingston, A. Bismarck, K. Li, Polyaniline hollow fibres for organic solvent nanofiltration, Chem. Commun. (2008) 6324–6326.
[26] I.F.J. Vankelecom, K. De Smet, L.E.M. Gevers, A. Livingston, D. Nair, S. Aerts, S. Kuypers, P.A. Jacobs, Physico-chemical interpretation of the SRNF transport mechanism for solvents through dense silicone membranes, J. Membr. Sci. 231 (2004) 99–108.
[27] S. Liu, W.K. Teo, X. Tan, K. Li, Preparation of $PDMS^{vi}$-Al_2O_3 composite hollow fibre membranes for VOC recovery from waste gas streams, Sep. Purif. Technol. 46 (2005) 110–117.
[28] F. Xiangli, Y. Chen, W. Jin, N. Xu, Polydimethylsiloxane, (PDMS)/ceramic composite membrane with high flux for pervaporation of ethanol–water mixtures, Ind. Eng. Chem. Res. 46 (2007) 2224–2230.
[29] F. Xiangli, W. Wei, Y. Chen, W. Jin, N. Xu, Optimization of preparation conditions for polydimethylsiloxane (PDMS)/ceramic composite pervaporation membranes using response surface methodology, J. Membr. Sci. 311 (2008) 23–33.
[30] G.O. Yahaya, Separation of volatile organic compounds (BTEX) from aqueous solutions by a composite organophilic hollow fiber membrane-based pervaporation process, J. Membr. Sci. 319 (2008) 82–90.
[31] G. Schock, A. Miquel, R. Birkenberger, Characterization of ultrafiltration membranes: cut-off determination by gel permeation chromatography, J. Membr. Sci. 41 (1989) 55–67.
[32] S.R. Reijerkerk, M.H. Knoef, K. Nijmeijer, M. Wessling, Poly(ethylene glycol) and poly(dimethyl siloxane): Combining their advantages into efficient CO_2 gas separation membranes, J. Membr. Sci. 352 (2010) 126–135.
[33] R. Baker, Membrane Technology and Applications, 2nd edition, John Wiley & Sons, Ltd., 2004.
[34] M. Mulder, Basic Principles of Membrane Technology, Kluwer Academic Publishers, Dodrecht/Boston/London, 2000.
[35] P.P.I. Voigt, T. Holborn, G. Dudziak, M. Mutter, A. Nickel, Ceramic nanofiltration membranes for applications in organic solvents, in: 9th Aachen Membrane Colloquium, Aachen, Germany pp. pOP 20-21-OP 20-11, 2003.
[36] Y.H See Toh, X.X. Loh, K. Li, A. Bismarck, A.G. Livingston, In search of a standard method for the characterisation of organic solvent nanofiltration membranes, J. Membr. Sci. 291 (2007) 120–125.
[37] H.J. Zwijnenberg, A standardized characterization method for solvent resistant nanofiltration membrane modules, in: ICOM Presentation, 2005.
[38] X.J. Yang, A.G. Livingston, L. Freitas Dos Santos, Experimental observations of nanofiltration with organic solvents, J. Membr. Sci. 190 (2001) 45–55.
[39] L.E.M. Gevers, I.F.J. Vankelecom, P.A. Jacobs, Zeolite filled polydimethylsiloxane (PDMS) as an improved membrane for solvent-resistant nanofiltration (SRNF), Chem. Commun. (2005) 2500–2502.